Cell Reports
Article

Cell PRESS
Open ACCESS

Transformed Epithelia Trigger Non-Tissue-Autonomous Tumor Suppressor Response by Adipocytes via Activation of Toll and Eiger/TNF Signaling

Federica Parisi,[1,2] Rhoda K. Stefanatos,[1,2] Karen Strathdee,[1] Yachuan Yu,[1] and Marcos Vidal[1,*]
[1]The Beatson Institute for Cancer Research, Garscube Estate, Switchback Road, Bearsden, Glasgow G61 1BD, UK
[2]These authors equally contributed to this work
*Correspondence: m.vidal@beatson.gla.ac.uk
http://dx.doi.org/10.1016/j.celrep.2014.01.039

SUMMARY

High tumor burden is associated with increased levels of circulating inflammatory cytokines that influence the pathophysiology of the tumor and its environment. The cellular and molecular events mediating the organismal response to a growing tumor are poorly understood. Here, we report a bidirectional crosstalk between epithelial tumors and the fat body—a peripheral immune tissue—in *Drosophila*. Tumors trigger a systemic immune response through activation of Eiger/TNF signaling, which leads to Toll pathway upregulation in adipocytes. Reciprocally, Toll elicits a non-tissue-autonomous program in adipocytes, which drives tumor cell death. Hemocytes play a critical role in this system by producing the ligands Spätzle and Eiger, which are required for Toll activation in the fat body and tumor cell death. Altogether, our results provide a paradigm for a long-range tumor suppression function of adipocytes in *Drosophila*, which may represent an evolutionarily conserved mechanism in the organismal response to solid tumors.

INTRODUCTION

Tumorigenesis is a very dynamic event that results in interactions between different cell types and the production of proinflammatory cytokines. In advanced cancers, which are characterized by a high tumor burden, transformed epithelial cells release chemokines and cytokines to recruit immune cells to the tumorigenic lesion. Currently accepted as a hallmark of cancer (Hanahan and Weinberg, 2011), tumor-related inflammation is a complex and not well-understood process. It has been suggested that a dynamic interaction between tumors and the immune system is essential for tumor survival, growth, and metastasis (Maruyama et al., 2011). However, studying the role of tumor-related inflammation in advanced cancers in vivo is complicated by the genetic redundancy of inflammatory cytokines and the ethical limitations of inflicting high tumor burden on conventional laboratory animals.

Studies using the fruit fly *Drosophila melanogaster* provided founding evidence for the existence of tumor suppressor genes, with the discovery of the *lethal (2) giant larvae* (*l(2)gl*) mutant in the 1920s (Stern and Bridges, 1926). The *scribble* (*scrib*) group of tumor suppressors, which includes the *l(2)gl*, *discs large* (*dlg*), and *scrib* genes, has been extensively characterized for its role in the establishment of apical basal polarity in epithelial cells (Bilder, 2004). Homozygous loss-of-function mutations of any of these genes are sufficient to disrupt epithelial architecture and lead to neoplastic transformation of mitotic tissues. Many studies have focused on tissue autonomous roles of the *scrib* group in tumorigenesis (Bilder et al., 2000; Bilder and Perrimon, 2000; Brumby and Richardson, 2003; Doggett et al., 2011; Dow et al., 2003; Froldi et al., 2008; Humbert et al., 2008; Wu et al., 2010). However, little is known about the effects that a growing tumor has on the physiology of the peripheral tissues. Previous work by colleagues and us indicates that hemocytes are recruited to neoplastic tumors, increase in number, and express Eiger/tumor necrosis factor (TNF)-α (Cordero et al., 2010; Pastor-Pareja et al., 2008). This suggested the existence of an interaction between tumors and the immune system. Moreover, it has been recently shown that tumors (like wounds) intersect the Ecdysone system to delay metamorphosis (Colombani et al., 2012; Cordero et al., 2010; Garelli et al., 2012). Reciprocally, the physiology of the host can influence tumors, because dietary sugar can affect tumor progression via Insulin signaling (Hirabayashi et al., 2013). Therefore, a complex crosstalk between growing tumors and the physiology of the animal is evident. Nevertheless, which are the different components of this systemic response and how they are connected remain unclear.

In this study, we systematically examined the response to tumor development in several tissues in *Drosophila*: the tumor itself, the hemocytes, and the fat body. We report a bidirectional communication between imaginal disc tumors and the fat body, which is integrated by the hemocytes. In the presence of tumors, the ligand Spätzle —produced by hemocytes— activates Toll/NF-κB signaling in the fat body. This activation within the fat body is, in turn, required to induce tumor cell death through

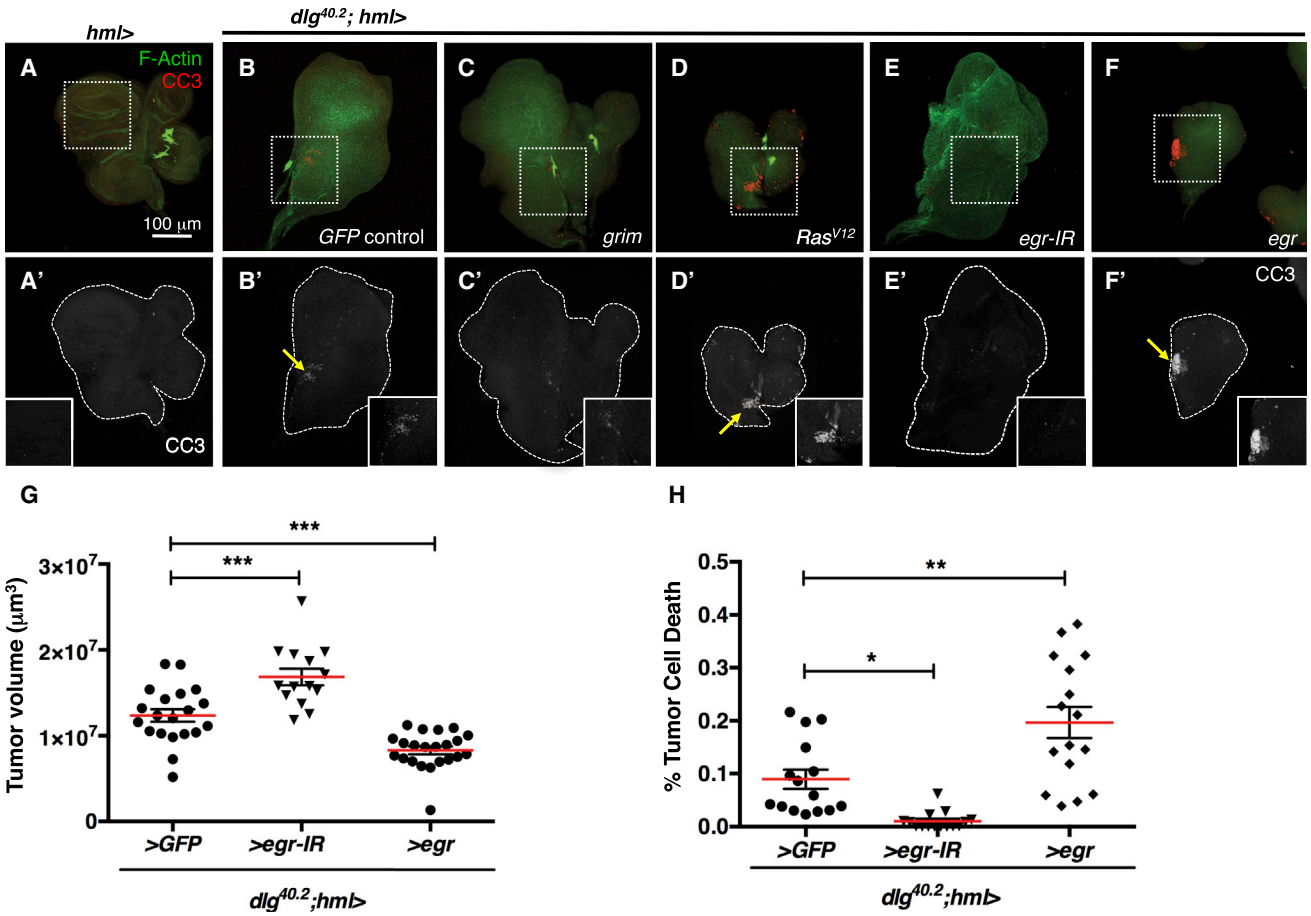

Figure 1. Tumor Cell Death Depends on Hemocyte-Derived Eiger

(A–F) Immunofluorescence of normal wing discs (A) or imaginal disc tumors (B–F) from $dlg^{40.2}$; *hml-gal4* larvae expressing *GFP* (B), *grim* (C), Ras^{V12} (D), an RNAi transgene for *eiger* (*egr-IR,* E), and *egr* (F), stained for F-actin (green) and anticleaved caspase 3 (CC3, red, gray in A′–F′; arrows point to regions of CC3 staining). (G and H) Quantifications of tumor volume (see Experimental Procedures; G, one-way ANOVA with Bonferroni post test correction, ***$p < 0.001$) and percentage volume of tumor with apoptotic cells (H, one-way ANOVA with Bonferroni post test correction, *$p < 0.05$ and **$p < 0.005$). Error bars represent SEM in these and subsequent figure panels.

See also Figures S1 and S2A–S2G.

hemocyte-derived Eiger. Altogether, our results define a cellular and molecular network mediating the systemic response to tumors and uncover a tumor suppressor role of the fat body through the activation of Toll signaling.

RESULTS

Hemocytes Directly Influence Tumor Size by Triggering Apoptotic Cell Death

Current evidence in *Drosophila* cancer models indicates that plasmatocytes, the phagocytic subtype of hemocytes (1) are recruited to tumors, (2) increase in number, and (3) express the *Drosophila* TNF-α ortholog (Cordero et al., 2010; Pastor-Pareja et al., 2008). To gain further understanding into the role of hemocytes, we introduced the hemocyte-specific driver *hemolectin-Gal4* (*hml-Gal4*) (Goto et al., 2001) into a $dlg^{40.2}$ mutant background (hereafter referred to as $dlg^{40.2}$; *hml* > *GFP*) and confirmed that *dlg* mutant larvae also displayed elevated numbers of circulating hemocytes (Figure S1A; see Experimental Procedures).

We tested whether, as in the case of *scrib* mutants (Pastor-Pareja et al., 2008), there was a functional effect of hemocyte number on *dlg* tumors. Increasing the number of hemocytes by overexpressing Ras^{V12} with *hml-gal4* resulted in smaller *dlg* imaginal disc tumors ($dlg^{40.2}$; *hml* > Ras^{V12}), whereas reducing hemocyte number by expressing the proapoptotic protein Grim ($dlg^{40.2}$; *hml* > *grim*) rendered larger tumors (Figures 1A–1D, S1B, and S1C).

Remarkably, manipulations of hemocyte number directly affected the levels of apoptotic cell death within tumors (Figures 1A–1D and S1D). Increased numbers of hemocytes in an otherwise wild-type background (*hml* > Ras^{V12}) did not affect growth, patterning, or the basal apoptotic rate observed in normal wing imaginal discs (Figures S2B and S2F). Together, the results indicate that hemocytes restrict tumor burden by inducing apoptotic cell death.

Tumor Cell Death Requires Hemocyte-Derived Eiger

We have previously demonstrated that Eiger (Egr) produced by the hemocytes is essential to trigger Egr signaling within tumor cells (Cordero et al., 2010). We next tested whether Egr expression in hemocytes was important for triggering tumor cell death. We specifically overexpressed or knocked down *egr* by RNAi in hemocytes of *dlg* mutants (*dlg*$^{40.2}$*; hml* > *egr* or *dlg*$^{40.2}$*; hml* > *egr-IR*, respectively). Tumors dissected from *dlg*$^{40.2}$*; hml* > *egr* larvae were significantly smaller and displayed increased cell death relative to control ones (*dlg*$^{40.2}$*; hml* > *GFP*). Critically, *dlg*$^{40.2}$*; hml* > *egr-IR* tumors were bigger than controls and displayed no signs of apoptosis (Figures 1E–1H). No defects were detectable when *egr* was overexpressed in the hemocytes of tumor-free control animals (Figures S2A and S2E), indicating that *egr* expression in hemocytes does not induce cell death in normal epithelial cells. Moreover, when we combined *Ras*^{V12} and *egr-IR* expression in hemocytes (*dlg*$^{40.2}$*; hml* > *Ras*^{V12}; *egr-IR*) *egr* knockdown was sufficient to compromise the tumor suppressor activity of hemocytes even in the presence of increased hemocyte number (Figures 2A–2D). Altogether, our results demonstrate that hemocyte-derived Egr exerts its tumor suppressive role through the induction of tumor cell death by apoptosis.

Immunolabeling of the Egr protein is observed as intracellular puncta within *scrib* and *dlg* tumor cells and at the plasma membrane of tumor-associated hemocytes (Cordero et al., 2010; Igaki et al., 2009). To further investigate the requirement of hemocyte-derived Egr for tumor cell death, we imaged a Venus-tagged form of Egr expressed in hemocytes of tumor-free animals or *dlg*$^{40.2}$ mutants (*he* > *egr*^{venus} or *dlg*$^{40.2}$*; he* > *egr*^{venus}). Hemocytes expressing *egr*^{venus} were found associated to wild-type imaginal discs, as well as imaginal disc tumors (Figures 2E–2H). However, we observed Venus-positive puncta outside hemocytes exclusively in tumor cells (Figures 2F and 2H; arrows). Across the imaginal disc tumors, the regions of Venus-positive puncta partly correlated with regions of apoptotic cell death, and numerous tumor cells displayed both Venus puncta and cleaved caspase staining (Figures 2H and S2H). This phenomenon was never observed in wild-type epithelia where Egr^{venus} was confined to the associated hemocytes (Figures 2E and 2G). Altogether, these results further indicate that hemocyte-derived Egr induces tumor apoptosis and restricts tumor growth via a non-cell-autonomous mechanism.

Eiger Is Required for Hemocyte Proliferation through Production of Pvf

We next looked into the mechanisms involved in the regulation of hemocyte proliferation in tumor-bearing larvae, which we found essential to trigger tumor cell death (e.g.; Figure 1). We observed that loss of *egr* was sufficient to decrease the number of circulating hemocytes in *scrib* tumor-bearing larvae (Figure 3A). *Drosophila* Pvfs are orthologs of vertebrate VEGF/PDGF and have been shown to drive hemocyte migration and proliferation in different contexts (Munier et al., 2002; Parisi and Vidal, 2011; Wood et al., 2006). Quantitative RT-PCR (qRT-PCR) on *scrib*^{1} imaginal discs demonstrated an increase in the expression of *pvf1* compared to *wild* type discs, which was dependent on *egr* (Figure 3B). Consistently, RNAi knockdown of the Pvf Receptor Pvr in hemocytes of *dlg* mutants using *hml-gal4* or *hemese-gal4* (*dlg*$^{40.2}$*; hml* > *Pvr-IR* or *dlg*$^{40.2}$*; he* > *Pvr-IR*) reduced the number of circulating hemocytes in *dlg* larvae (Figures 3C and S3A). We next tested the functional relevance of Pvf1/Pvr signaling from hemocytes in tumor development. We found a significant increase in the size of *dlg*$^{40.2}$*; hml* > *Pvr-IR* tumors compared to controls (Figure 3D–3F). Consistent with our previous results, the increase in tumor size was correlated with reduced levels of cell death in *dlg*$^{40.2}$*; hml* > *Pvr-IR* tumors (Figures 3D, 3E, and 3G).

Taken together, these results indicate that Eiger signaling within the epithelial tumor impacts the host systemically through upregulation of Pvf1, which signals in hemocytes through its receptor Pvr to drive hemocyte proliferation.

Tumor-Bearing Larvae Display Toll Activation in the Fat Body

Given the systemic effects of tumors on hemocyte number, we hypothesized that the fat body, which also plays a key role in *Drosophila* innate immunity (Hoffmann, 1995), could be an active component of the organismal response to tumors. We therefore used reporter lines and qRT-PCR to screen for activation of pathways previously implicated in immunity such as the Immune Deficient/Relish (IMD/Rel), Insulin Receptor (InR/FoxO), Egr/JNK, and Toll/NF-κB pathways within adipocytes. We further tested whether these candidate pathways were activated in a non-tissue-autonomous manner (i.e.; activated in adipocytes from both zygotic mutant larvae as well as in larvae containing eye imaginal disc tumors but otherwise wild-type; see the Experimental Procedures). Using these criteria, we failed to detect any significant change in the fat body activity of IMD/Rel, InR/FoxO, and Egr/JNK pathways (Figures S4A–S4I). However, the expression of a Toll/NFκB pathway reporter, *drosomycin* (*drs*) (Ferrandon et al., 1998), was dramatically upregulated in the fat body of most zygotic *scrib*^{1} and *l(2)gl* mutant larvae (Figures 4A–4F) as well as in larvae-bearing *Ras*^{V12}*; scrib*^{1} eye imaginal disc tumors (Figure 4J). Similarly, we observed fat body upregulation of *defensin*, an independent Toll target (Figure S4K).

drs-GFP was still upregulated in the fat body of *scrib*^{1} mutant larvae raised in germ-free-like conditions (Figures 4G–4I; see Experimental Procedures), suggesting that Toll pathway upregulation in the fat body was indeed due to the presence of tumors and not secondary to pathogenic infection. Finally, we failed to detect Toll signaling activation in the fat body of developmentally arrested *ecd*^{1} mutants (Figure 4J), indicating the effect was not a result of developmental delay.

Altogether, these results suggest a direct influence of developing *Drosophila* epithelial tumors on the adipose tissue, which is manifested by the activation of Toll signaling in the latter.

Hemocytes Are Essential Mediators of the Crosstalk between Tumors and the Fat Body

The secreted ligand Spätzle (Spz) binds to the Toll receptor and activates downstream signaling during the immune response to infection (Shia et al., 2009) (Lemaitre and Hoffmann, 2007).

We next tested a potential role of hemocyte-derived Spz in the activation of Toll in the fat body of tumor-bearing larvae. Targeted knockdown of Spz within hemocytes by RNAi

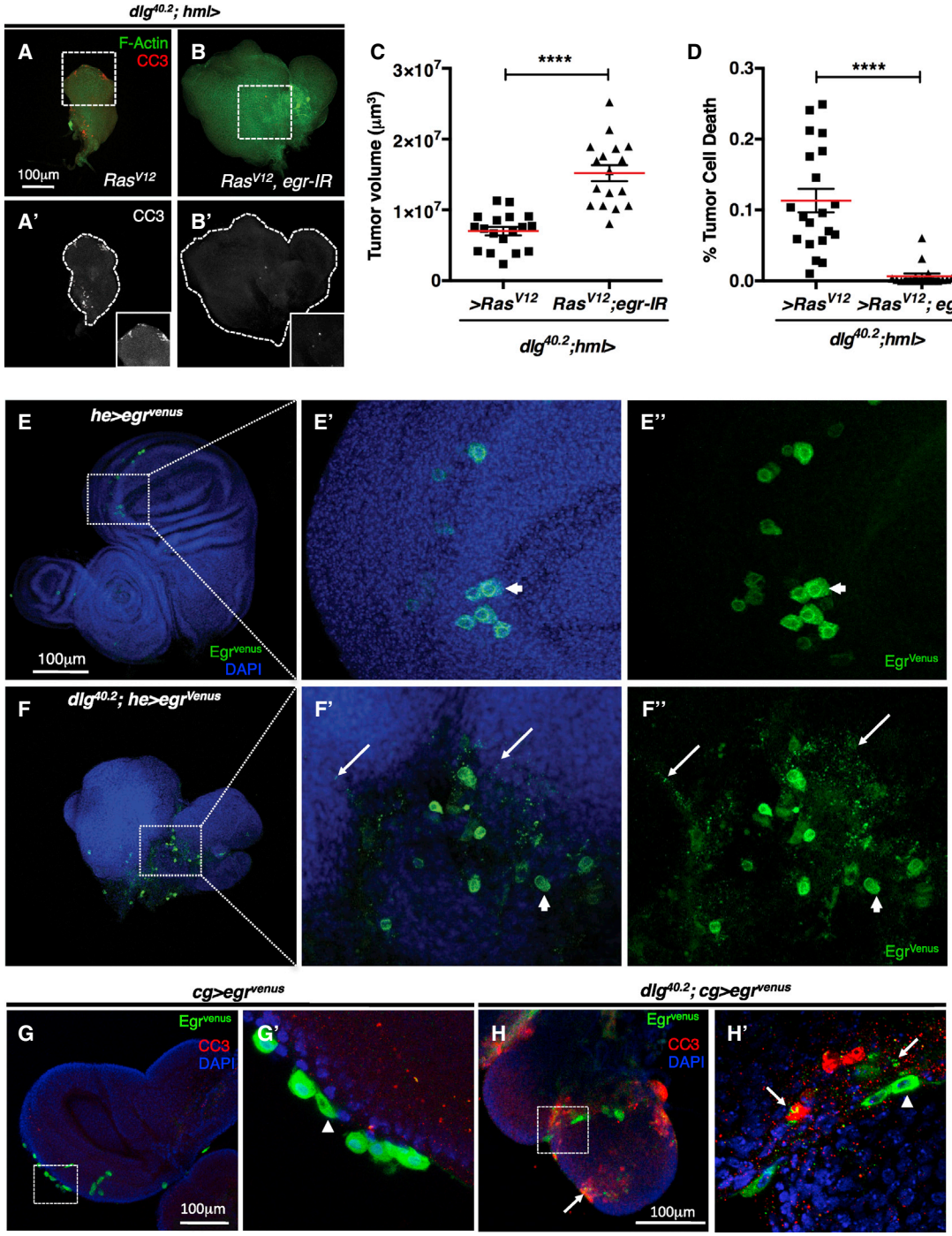

Figure 2. Hemocyte-Derived Eiger Is Incorporated into Tumor Cells

(A and B) Immunofluorescence of tumors from *dlg*$^{40.2}$*; hml-gal4* larvae expressing *Ras*^{V12} alone (A) or in combination with *egr* RNAi (*Ras*^{V12}*; egr-IR*, B), which were stained for F-actin (green) and CC3 (red and gray in A′ and B′).

(C and D) Quantification of tumor volume (C, t test ****p < 0.0001) and percentage volume of tumor with apoptotic cells (D, t test ****p < 0.0001).

(E and F) Control wing disc (E) and *dlg*$^{40.2}$ tumor (F) from larvae expressing *UAS-egr*^{venus} under the control of *he-gal4*. Arrowheads point to tissue associated hemocytes; arrows point to Egr-Venus puncta located within epithelial tumor cells. (E′)–(F″) show a high-magnification view from the boxed areas in (E) and (F).

(G and H) Control wing discs (G) and wing disc tumors from *dlg*$^{40.2}$ larvae (H) expressing *UAS-egr*^{venus} under the control of *cg-gal4* and stained with anticleaved caspase 3. Arrowheads and arrows are as in (F′). Note that the regions of Egr^{venus} positive puncta were often seen within regions of caspase activation (arrows) and pycnotic nuclei (not shown). (G′)–(H′) show high-magnification view from the boxed areas in (G) and (H).

See also Figure S2H.

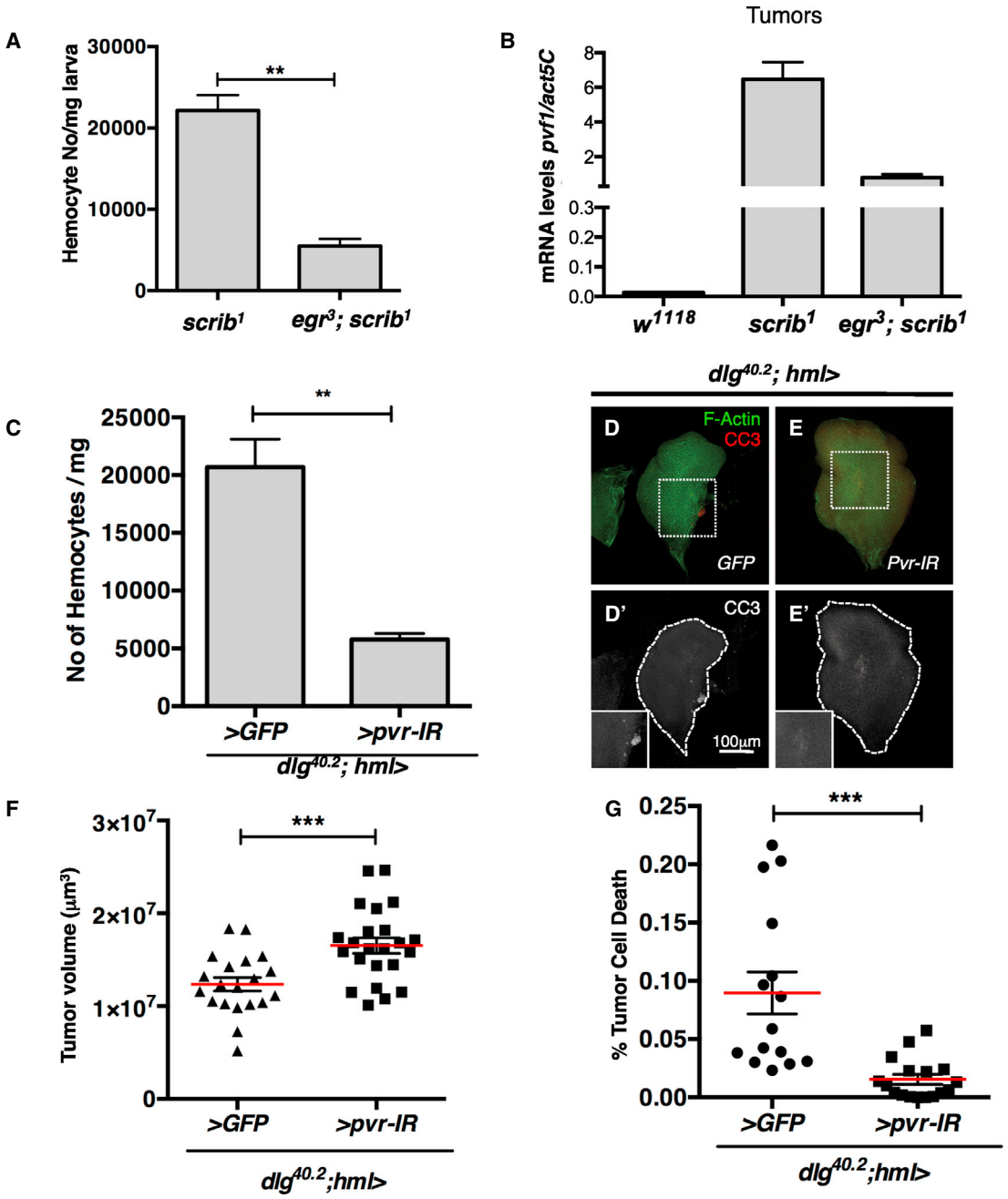

Figure 3. Eiger Drives Hemocyte Proliferation via Pvf1 to Restrict Tumor Growth

(A) Quantification of hemocyte density from the indicated genotypes (t test **p = 0.0013).

(B) qRT-PCR of *pvf1* in WT wing discs and wing disc tumors dissected from the genotypes indicated.

(C) Hemocyte density was quantified in the indicated genotypes (t test **p = 0.0011). Note the decrease in hemocyte number in animals with hemocyte-specific knockdown of *pvr* achieved with *hml-gal4*.

(D and E) Immunofluorescence of tumors from $dlg^{40.2}$; *hml-gal4* larvae expressing *GFP* or *pvr-IR* as indicated and stained for F-actin and CC3.

(F and G) Quantifications of tumor volume (F, t test ***p = 0.0006) and percentage volume of tumor with apoptotic cells (G, t test ***p = 0.0002).

See also Figure S3.

($dlg^{40.2}$; *hml>spz-IR*) resulted in reduced Toll activation in the fat body of *dlg* mutants, as indicated by qRT-PCRs for *drs* mRNA (Figure 4K). Consistent with the production of the Toll ligand Spz by hemocytes, expanding the population of hemocytes by overexpressing Ras^{V12} enhanced Toll reporter activation in the fat body ($dlg^{40.2}$; *hml* > Ras^{V12}; Figure 4K).

Together these results indicate that tumor-driven activation of Toll signaling in the fat body is mediated by hemocyte secretion

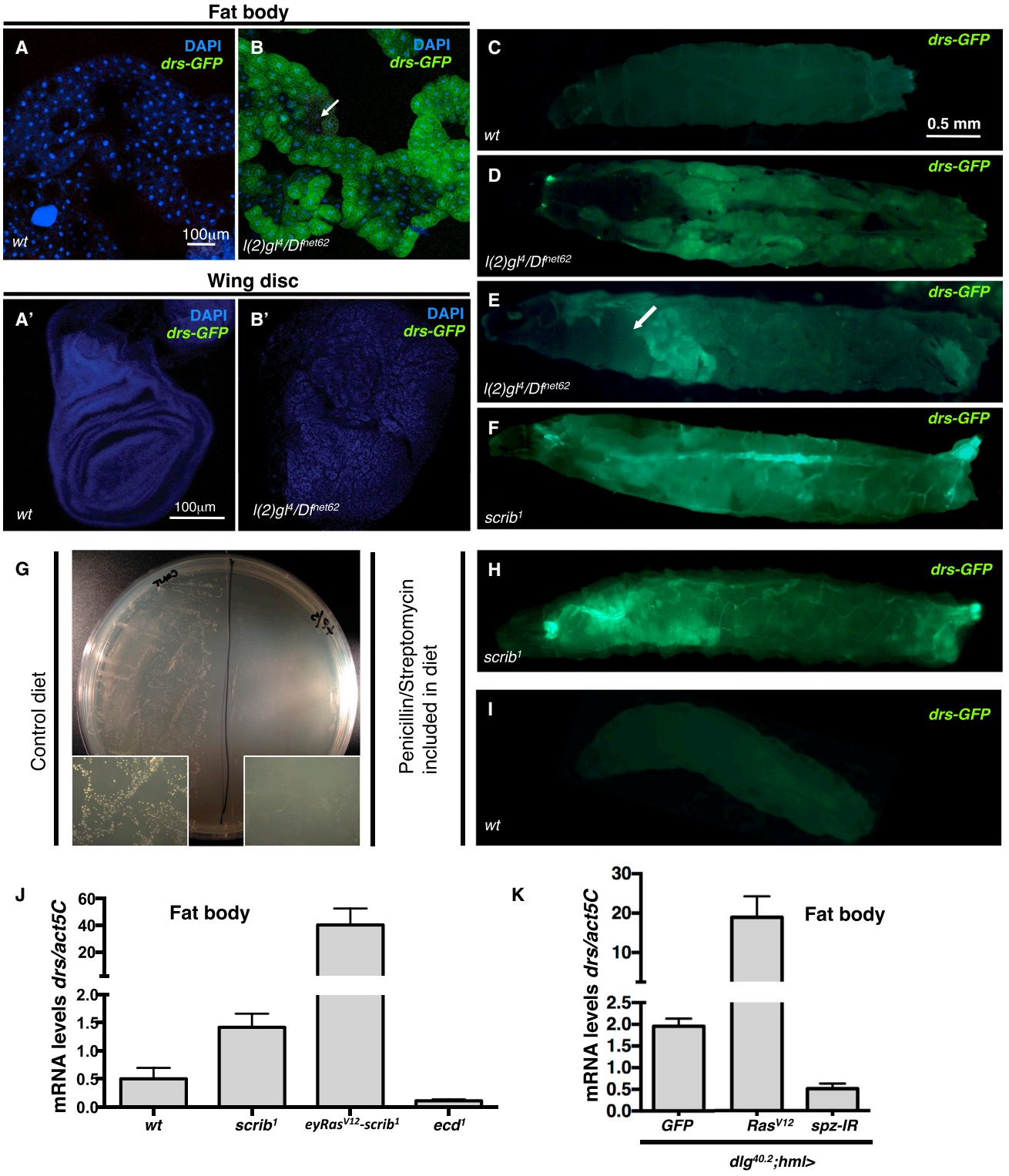

Figure 4. Tumor-Bearing Larvae Display Toll Pathway Activation in Their Fat Body

(A and B) *drosomycin-GFP* (*drs-GFP*, green) fluorescent signal (counterstained with DAPI for nuclei in blue) from dissected fat bodies (A and B) or wing discs (A′ and B′) from wild-type controls (WT) and mutants for *lethal (2) giant larvae* (*l(2)gl*^{4}*/Df*^{net62}). Note that, in *lgl*^{4} mutants, the *drs-GFP* reporter was activated in the fat body in a patchy manner (arrow in B points to an adipocyte with relatively lower levels of drs-GFP expression) but not in the imaginal disc tumors (B′).

(legend continued on next page)

of Spz and points to hemocytes as a link for long-range sensing of tumor burden by the immune system.

Tumor-Intrinsic Egr Activates Toll in the Fat Body

Having established that Egr signaling within the tumors is required for hemocyte proliferation (Figure 3A) and that hemocyte-derived Spz is necessary for Toll activation in the fat body (Figure 4K), we next tested whether there was a functional connection between Egr and Toll activation. Remarkably, the upregulation of *drs* in the fat body of *scrib*^{1} larvae was prevented upon systemic loss of *egr* (*egr*^{3}*; scrib*^{1}; Figures 5A–5C).

We next tested whether tumor- and/or immune tissue-derived Egr was required for Toll activation in the fat body. Overexpression or RNAi knockdown of Egr in both hemocytes and the fat body using *cg-gal4* (*dlg*$^{40.2}$*; cg > egr* or *dlg*$^{40.2}$*; cg > egr-IR*) did not modify *drs* mRNA levels (Figure 5D). Moreover, reducing or enhancing expression of Egr specifically in hemocytes (*dlg*$^{40.2}$*; hml > egr-IR* or *dlg*$^{40.2}$*; hml > egr*) did not significantly affect *drs* mRNA in the fat body of *dlg* mutants (Figure 5E). These results suggest that a source of Egr distinct from the hemocytes and the fat body itself is responsible for this Egr-dependent Toll activation in adipocytes. To test the role of tumor-derived Egr in this process, we cosilenced *dlg* and *egr* in the wing pouch using *scalloped (sd)-gal4* driver. Consistent with our previous observations, *dlg* knockdown in the *sd* domain was sufficient to trigger activation of Toll signaling in the fat body (*drs-GFP/sd > dlg-IR;* Figures 5F and 5F′). Importantly, this effect was never observed in fat bodies from *drs-GFP/sd > dlg-IR; egr-IR* larvae, even though the wing disc pouches displayed increased overgrowth (Figures 5G and 5G′).

Altogether, these results indicate that *egr* expression within epithelial tumors is required to activate Toll in the fat body.

Toll Signaling Restrains Tumor Growth in a Non-Tissue-Autonomous Manner

We next addressed the functional relevance of Toll signaling activation in the fat body of *dlg* larvae. First, we noted that Spz silencing in hemocytes (*dlg*$^{40.2}$*; hml > spz-IR* or *dlg*$^{40.2}$*; he > spz-IR*) resulted in increased tumor size and decreased tumor cell death (Figures 6A–6D and S5A–S5D). We then modulated Toll signaling in the fat body using the *pumpless-Gal4* (*ppl-Gal4*) driver (Zinke et al., 1999). Tumors from larvae with impaired Toll activation in the fat body achieved through RNAi for the Toll adaptor protein Myd88 (*dlg*$^{40.2}$*; ppl > Myd88-IR*) were significantly bigger and displayed reduced cell death when compared to controls tumors (Figures 6G, 6I, and 6J). These results were confirmed by silencing *Myd88* with two independent fat body drivers (*cg-gal4* and *lsp2-gal4*) (Figures S5F–S5K). Conversely, enhanced Toll activation in the fat body achieved by overexpression of wild-type Toll receptor (*dlg*$^{40.2}$*; ppl > Toll*) resulted in decreased tumor volume and increased tumor cell death (Figures 6H–6J). A similar overexpression of Toll in tumor-free animals did not cause ectopic cell death or patterning defects in normal discs (Figures S2C and S2G). Finally, inhibiting Toll specifically within hemocytes showed no detectable effect on either tumor burden or tumor cell death (Figure S5E).

Taken together, these data indicate that the innate immune system can restrict tumor growth in a non-tissue-autonomous manner through activation of Toll signaling in the fat body.

Hemocyte-Derived Egr Is Necessary to Execute Toll-Dependent Tumor Cell Death

Finally, given the correlation observed among hemocyte number, Toll signaling activation in the fat body, and tumor cell death, we next tested whether hemocyte-derived Egr was required to execute tumor cell death downstream of Toll activation. We used *cg-gal4* to overexpress Toll in both hemocytes and the fat body, while simultaneously knocking down *egr*. Overexpression of *Toll* (*dlg*$^{40.2}$*; cg > Toll*) decreased tumor size and enhanced tumor cell death (Figures 7A, 7C, and 7D; compare with Figures S5H and S5I). Remarkably, concomitant overexpression of *Toll* and knockdown of *egr* (*dlg*$^{40.2}$*; cg > Toll; egr-IR*) strongly suppressed apoptotic tumor cell death and increased tumor size (Figures 7B–7D). The knockdown of *egr* in the immune tissues, however, did not affect the enhanced expression of the Toll target *drs* in the fat body of *dlg*$^{40.2}$*; cg > Toll; egr-IR* larvae (Figure 7E). These results suggest hemocyte-derived Egr is required downstream of Toll signaling in the fat body to execute epithelial tumor cell death.

DISCUSSION

In this study, we have investigated the systemic interaction between the fat body and developing tumors. These data uncover a non-tissue-autonomous role for *Drosophila* adipocytes in the control of tumor growth. This is achieved through a relay of the Pvf1/Pvr, Spz/Toll, and Eiger signaling pathways (model in Figure 7F).

Adipocytes Restrain Tumor Burden via Toll Signaling

Research in *Drosophila* has made seminal contributions to the understanding of innate immune signaling. The discovery of the role of Toll-like receptors (TLRs) in innate immunity was first made in the fruit fly and was rapidly followed by the characterization of their relationship with NFκB signaling (Lemaitre,

(C–F) Whole larva micrographs showing *drs-GFP* in WT (C), *l(2)gl*^{4}*/Def* (E and F), and *scrib*^{1} (F). The arrow in (E) points to transformed discs, negative for *drs-GFP* signal. The larva in (E) was 9–10 days old and in (D) 11–12 days old.

(G) Demonstration of germ-free-like conditions using antibiotics (see Experimental Procedures). Animals were raised in control diet (left side of plate) or penicillin/streptomycin (P/S) containing diet (right side of plate) and homogenized and spread on antibiotic-free LB plates.

(H and I) *drs-GFP* signal from animals raised in P/S treated diet from the indicated genotypes. Note that *scrib*^{1} mutant larvae displayed reporter activation even when raised in germ-free-like conditions.

(J and K) qRT-PCR for *drs* mRNA from dissected fat bodies from the indicated genotypes. All animals were 11 days old except the WT controls, which were 5 days old. Note that *drs* was upregulated in *scrib*^{1} mutant larvae as well as in larvae carrying eye disc-only tumors (*eyRas*^{V12}*-scrib*^{1}; see Experimental Procedures); *ecd*^{1} mutant larvae who arrest at the larval stage as tumor-bearing larvae but are free of tumors displayed low levels of *drs* (J). Expressing *Ras*^{V12} or silencing *spätzle* (*spz*) in the hemocytes of *dlg* mutant larvae upregulated and downregulated *drs* levels, respectively (K).

See also Figure S4.

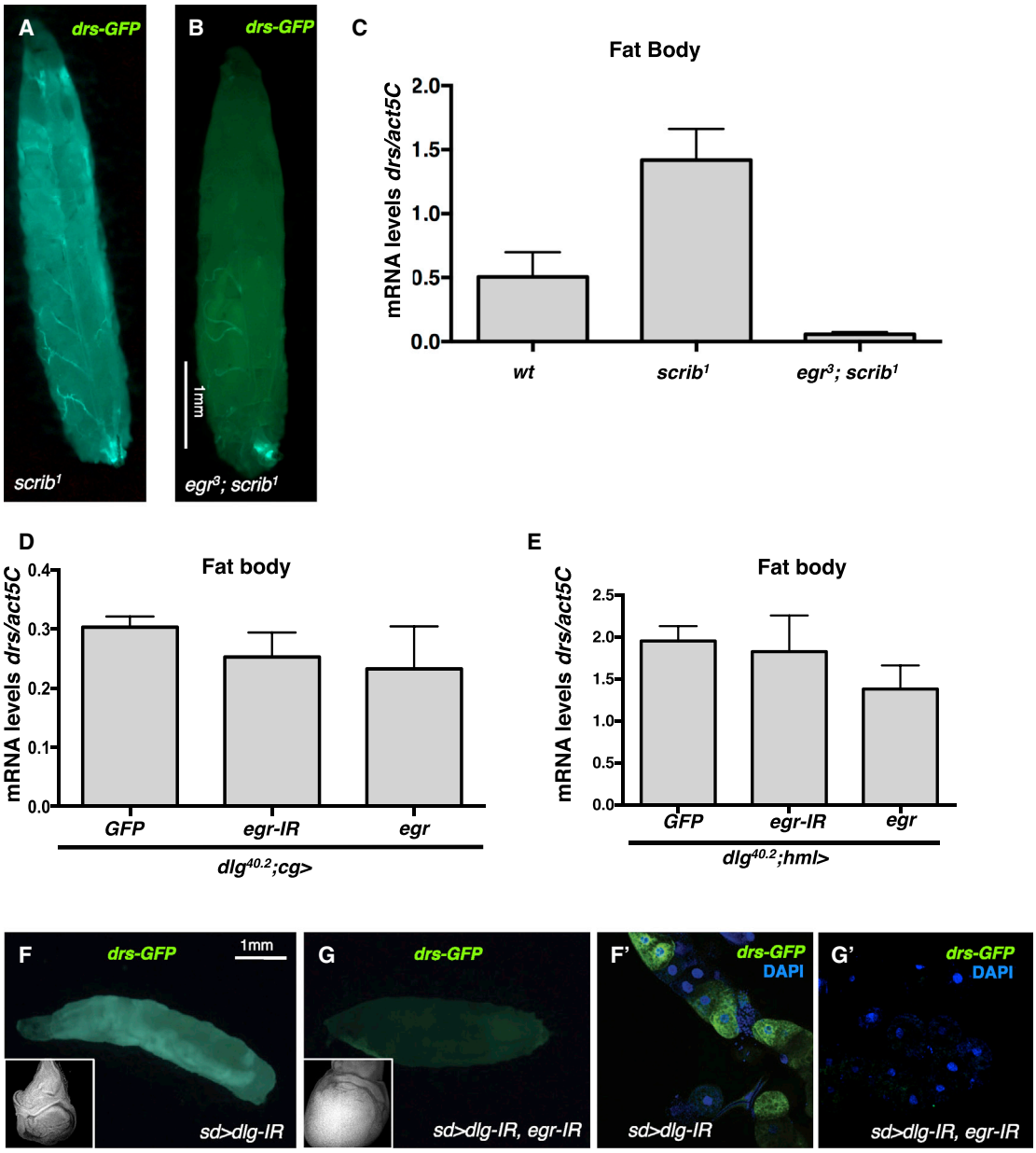

Figure 5. Eiger Is Upstream of Toll Activation in the Fat Body

(A and B) Micrographs from *scrib*^{1} and *egr*^{3}*; scrib*^{1} larvae in the genetic background of the Toll reporter *drs-GFP*.

(C) qRT-PCR for *drs* from fat bodies of WT, *scrib*^{1}, and *egr*^{3}*; scrib*^{1} larvae. Note that *drs* expression depended on *egr*.

(D–E) qRT-PCR for *drs* in dissected fat bodies from *dlg* larvae expressing *GFP*, *egr-IR*, or *egr* under the control of *hml-* or *cg-gal4*. Note that modulating *egr* expression levels in hemocytes or the fat body itself did not affect the levels of *drs* expression in the fat body of *dlg* mutants.

(F and G) Fluorescent micrographs from whole larvae (F and G) and dissected fat bodies (F' and G') from animals expressing *dlg-IR* alone or in combination with *egr-IR*, under the control of *sd-gal4* in the genetic background of *drs-GFP*. Note that whereas the overgrowth of the *dlg* deficient wing pouch was exacerbated by *egr* cosilencing (insets in F and G, DAPI staining in gray), the cosilencing of *egr* prevented the activation of *drs-GFP* in the fat body.

2004). These studies led to the identification of mammalian TLRs counterparts and their function in both the innate and adaptive immune responses (Akira, 2003; Beutler et al., 2003).

Mammalian TLRs are important mediators of cancer-related inflammation (Karin and Greten, 2005; Maruyama et al., 2011). Nevertheless, the mechanisms that activate TLR signaling in cancer remain poorly understood. Some evidence suggests that injured or necrotic cells release molecules not normally found in the extracellular milieu (e.g., DNA and nuclear proteins) that act as endogenous ligands for pattern recognition receptors like TLRs (Kim and Karin, 2011). However, it is difficult to test genetically the role in vivo of these molecular factors.

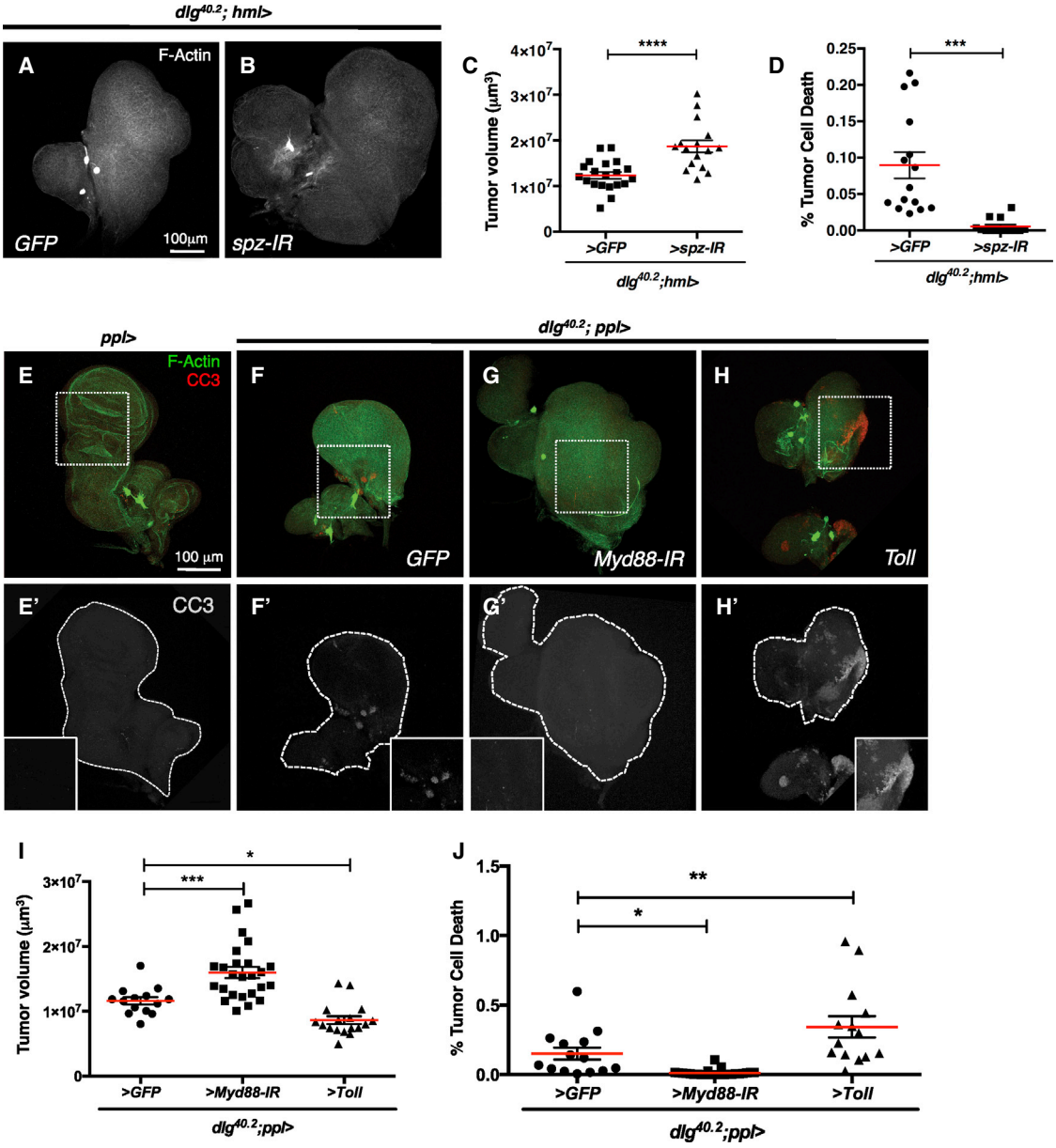

Figure 6. Toll Activation in the Fat Body Remotely Controls Tumor Growth

(A and B) F-Actin stained *dlg* imaginal disc tumors from the indicated genotypes. Note that silencing *spz* in the hemocytes of *dlg* mutant larvae resulted in enlarged tumors.

(C and D) Quantification of tumor volume and percentage of volume with apoptotic cells (C, t test ****$p < 0.0001$ and D, ***$p = 0.0001$). See also Figure S5.

(E–H) Control imaginal disc and imaginal disc tumors from *dlg*$^{40.2}$*; ppl-gal4* larvae expressing *GFP* (F), *Myd88-IR* (G), or *Toll* (H) and stained for F-actin (green) and CC3 (red or gray in bottom panels).

(I–J) Quantifications of tumor volume and percentage of tumor volume with apoptotic cells from the indicated genotypes (one-way ANOVA with Bonferroni post test correction, *$p < 0.05$; **$p < 0.005$, ***$p < 0.001$, ****$p < 0.0001$).

Note that tumor size is inversely correlated with the levels of Toll signaling in the fat body, whereas the level of tumor cell death correlates directly with Toll activation.

During pathogen infection fly hemocytes produce the Toll ligand Spätzle to activate Toll signaling in the fat body (Shia et al., 2009). Remarkably, our results implicate Spz in the tumor recognition mechanism: *spz* knockdown in hemocytes resulted in reduced activation of Toll signaling in the fat body, decreased tumor cell death, and increased tumor burden. This study suggests the existence of a long-range, intertissue crosstalk between tumors and adipocytes that requires the hemocytes as messengers to activate Toll/NFκB signaling in the adipocytes and to restrain tumor growth.

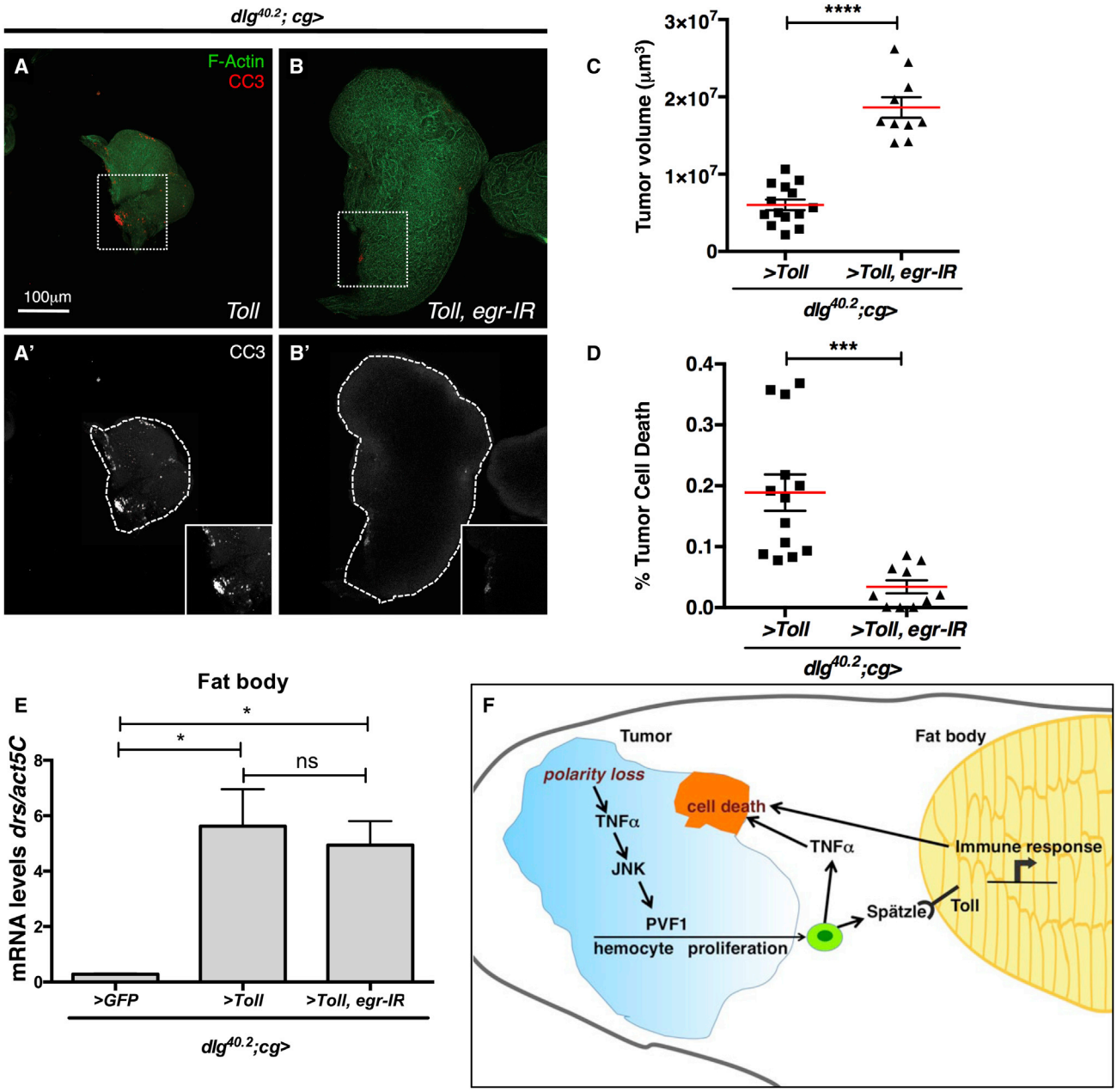

Figure 7. Toll Activation Requires Eiger to Control Tumor Growth

(A and B) Imaginal disc tumors from *dlg*$^{40.2}$*; cg-gal4* larvae expressing *Toll* alone (A) or in combination with *egr-IR* (B) stained for F-actin (green) and CC3 (red or gray in bottom panels).

(C and D) Quantification of tumor volume and percentage of volume with apoptotic cells in the indicated genotypes (C, t test ****$p < 0.0001$ and D, ***$p = 0.0003$). Note the increase in tumor volume and the decrease in tumor cell death when *egr* was silenced together with Toll overexpression using the *cg-gal4* driver.

(E) qRT-PCR for *drs* in dissected fat bodies from *dlg* larvae expressing either *GFP* or Toll alone or in combination with *egr-* under the control of *cg-gal4* (one-way ANOVA with Bonferroni post test correction, ns: nonsignificant and *$p < 0.05$). Note that overexpression of Toll resulted in enhanced production of *drs*, which was not affected by simultaneously silencing *egr*.

(F) A model for the two-way communication of epithelial tumors and the fat body. See the text for details.

Eiger and Hemocytes in the Immune Modulation of Tumor Growth

Since Virchow's first observations, the infiltration of blood cells has been appreciated as a common feature of solid tumors (Balkwill and Mantovani, 2001). Previous studies on the role of tumor-associated hemocytes in *Drosophila* indicate that hemocyte number correlates inversely with tumor growth (Pastor-Pareja et al., 2008) and that hemocytes are recruited from the

circulation into imaginal disc tumors and express *egr* (Cordero et al., 2010).

Here we provide additional evidence for a tumor-suppressor role for the hemocytes in *scribble* group mutant larvae: (1) functional manipulations of hemocyte number correlated with tumor cell death, (2) *egr* expression in hemocytes promoted cell death in epithelial tumor cells but not in normal cells, and (3) hemocytes released Venus-labeled Egr on imaginal disc tumors, and this correlated with apoptosis. This response to tumors requires Egr to be expressed both by tumor cells and hemocytes. Indeed, hemocyte-derived Egr was required for tumor cell death. Tumor-intrinsic expression of Egr might be required for systemic effects achieved via its target Pvf1, which mediates hemocyte proliferation. In turn, hemocyte proliferation results in increased production of Spz that activates Toll in the fat body.

Recent work demonstrated that tumors and wounds upregulate the Insulin-like peptide Dilp8, which prevents Ecdysone production to delay pupariation (Colombani et al., 2012; Garelli et al., 2012). We found that this upregulation was dependent on *egr*, and that overexpression of *egr* in the wing disc pouch was sufficient to upregulate *dilp8* (Figure S3).

Together, these data highlight a central role of Eiger expression both in tumor cells and hemocytes, for the host response to tumors.

A Functional Relationship of Egr/TNF and Toll Signaling

In mammals, TNF-α is a well-characterized TLR/NF-κB target, expressed in inflammatory conditions during infection and cancer (Balkwill, 2009). In response to tumor burden, our genetic data place Eiger both upstream and downstream of Toll signaling. In fact, systemic loss of *eiger* or silencing *eiger* in epithelial tumor cells inhibited Toll pathway activation in the fat body. Conversely, the non-tissue autonomous tumor suppressing effect of Toll via tumor cell death required *eiger* expression in the immune tissues. Therefore, Eiger and Toll signaling cooperate in a feedforward systemic response to tumor development. In mammalian systems, inflammatory cytokines such as TNF-α have been implicated in the systemic effects of high tumor burden (Balkwill, 2009). Future studies should explore whether Toll-like receptors are also involved, in particular, in tissues analogous to the fat body such as the white adipose tissue and liver.

EXPERIMENTAL PROCEDURES

Drosophila Stocks

A list of all fly stocks used and their sources can be found in Table S1.

Fly Husbandry and Genetics

Crosses were performed at 22°C in standard oatmeal and molasses medium (Fernandez-Ayala et al., 2009) and kept in incubators with a controlled 12 hr light/dark cycle. Crosses were performed in bottles with a controlled number of females and males and allowed to mate for a maximum of 2 days in order to control population density. Unless otherwise indicated, tumor-bearing larvae and ecd^{1} mutants were dissected 11 days after egg laying (AEL) for tumor, hemolymph, or fat body collection; wild-type-like control larvae were dissected at the wondering third instar stage. Gal-4 drivers were crossed into a $dlg^{40.2}$ background and combined with a UAS-GFP transgene. Larvae were examined for GFP fluorescence, and the expression pattern of each Gal-4 driver is shown in Table S2. The expression pattern of *sd-gal4* was examined in a wild-type background and can also be found in Table S2.

Immunofluorescence

Tissues were dissected in PBS and fixed 30 min in 4% paraformaldehyde (Polysciences). After fixation, samples were washed three times in PBS + 0.3% Triton X-100 (PBST) and incubated in primary antibodies and DAPI (Sigma-Aldrich) overnight at 4°C. Samples were washed as previously described and subjected to secondary antibody staining for 1–2 hr at room temperature followed by washing and mounting on Vectashield (Vector Laboratories) using Secured-Seal spacers (Life Technologies) to preserve the thickness of the tissues. Primary and secondary antibodies were incubated in PBST + 3% BSA. Primary antibodies used included rabbit anticleaved caspase 3 (1:200; Cell Signaling Technology), rabbit anti-βgal (1:1,000, Cappel antibodies) mouse anti-MMP1 (1:10; DSHB), and mouse anti-p1/Nimrod (1:5; kind gift of I. Ando). Phalloidin 594/647 was used to visualize the cytoskeleton (1:200/1:40; Life Technologies). Secondary antibodies used were Alexa 488, 594 (1:200; Life Technologies). Confocal images were captured using a Zeiss 710 confocal microscope and processed with ImageJ or Adobe Photoshop CS.

qRT-PCR Analysis

Each total RNA sample was extracted from 10–15 fat bodies or 30 tumors (in biological triplicates) using the QIAGEN RNeasy kit according to manufacturer's instructions. cDNA synthesis was performed using the High-Capacity cDNA Reverse Transcription Kit (Applied Biosystems). PerfeCTa SYBR green (Quanta Biosciences) was used for qRT-PCR following manufacturer's instructions. A series of 10-fold dilutions of an external standard was used in each run to produce a standard curve. cDNA was analyzed in triplicate using an Applied Biosystems 7500 fast instrument. mRNA levels for the relevant targets were measured using primers pairs shown in Table S3, and *actin5C* was used to normalize target expression levels. Data were extracted and analyzed using Applied Biosystems 7500 software version 2.0 and Prism GraphPad software. Data are presented as mean mRNA levels with SEM.

Statistics

Results are presented as scatter plots or bar graphs created using GraphPad Prism 6. A combination of t test and one-way ANOVA with Bonferroni's multiple comparison test was used to calculate statistical significance. p values are included in the relevant figure legends.

Quantification of Tumor Volume and Tumor Cell Death

Tumor volume was quantified from total volume of DAPI on confocal image series of tumors of all shown genotypes using the Volocity 3D imaging analysis software (PerkinElmer). For each tumor, 40–50 stacks were taken (2.55 μm/stack) and were used to render a 3D image; an example is shown in Movie S1. In most cases, the tumors derived from haltere or leg discs remain associated with the ones derived from wing discs; these are easily distinguishable in a $dlg^{40.2}$ background and were not considered for the quantifications.

Tissues stained for DAPI and cleaved caspase 3 (CC3) were used to quantify the level of cell death. Volocity 3D software was used to calculate the volume of the tumor positive for cleaved caspase 3 and was then normalized to total tumor volume (visualized by DAPI staining) to calculate the percentage tumor cell death. Twelve to 25 tumors were analyzed for each genotype.

Hemocyte Quantifications

Larvae were washed three times in PBS to remove any food debris. Five larvae per genotype were then opened and turned inside out using no. 5 forceps (Dumont) in 500 μl of PBS. The sample was gently pipetted to ensure equal distribution and avoid clustering, and 10 μl was loaded into each end of a hemocytometer (Bright Line), and the number of hemocytes were counted. The total number of hemocytes per larva was then calculated. To account for the increase in larval size, the number of hemocytes per larvae was normalized to the increase in hemolymph weight in tumor-bearing larvae. This ensured that differences in hemocyte number were not a result of increased hemolymph but rather an increase in hemocyte density/concentration. To measure larval weight, at least 15 larvae per genotype were pulled together in a preweighed Eppendorf tube, and their weight was measured on a high-precision scale (APX-100, Denver Instrument). These experiments were performed at least in triplicate for each genotype.

Generation of Eye Disc Tumors

In order to test whether the effects in the fat body of zygotic *scrib* or *dlg* mutants was a response to tumors versus a tissue autonomous effect of the *dlg* or *scrib* mutation, we used a MARCM system-derived tumor model (Pagliarini and Xu, 2003) in which clones of *scrib*^{1} mutant cells that also overexpress the Ras^{V12} oncogene are created specifically in the eye-antenna discs using the tissue specific *ey-FLP* recombinase (referred to as *eyRas*^{V12}*-scrib*^{1} larvae). In this case, every tissue, except the eye disc-derived tumors, is heterozygous for *scrib* and wild-type-like.

Whole Larva and Adult Wing Imaging

Third instar larvae were washed in dH_20, dried, and immobilized on double-sided tape. Images of were taken using a Leica M205 FA stereomicroscope. Adult wings were washed in PBS-T and mounted in 50% glycerol in PBS-T, and images were obtained with an Olympus BX51 microscope using a 5× lens.

Germ-free-like Conditions

The use of antibiotics was as previously described (Ridley et al., 2013). Briefly, embryos of *drs-GFP; scrib*^{1} larvae were raised in diet containing penicillin and streptomycin (100 IU/ml and 100 μg/ml, respectively, Gibco). After they developed as giant larvae, larvae were imaged for GFP signal. To confirm the germ-free-like conditions, single larvae were homogenized in 30 μl of sterile PBS, spread on antibiotic-free Luria-Bertani (LB) plates (animals raised in normal diet were spread in the same plate as internal controls), and incubated at 29°C for 48 hr.

SUPPLEMENTAL INFORMATION

Supplemental Information includes six figures, three tables, and one movie and can be found with this article online at http://dx.doi.org/10.1016/j.celrep.2014.01.039.

ACKNOWLEDGMENTS

We thank J. Cordero for editing the manuscript. We also thank our colleagues G. Davies, E. Martin-Blanco, S. Valenna, D. Hultmark, I. Anderl, G. Morata, M. Miura, T. Igaki, M. Uhlirova, C. Murgia, R. Patel, F. Leiler, D. Grifoni, P. Ligoxygakis, D. Bilder, B. Lemaitre, P. Leopold, I. Ando, and D. Ferrandon for reagents and/or advice, the VDRC and Bloomington stock centers and the Developmental Studies Hybridoma Bank for providing fly lines and antibodies, D. Strachan and M. O'Prey for assistance with imaging software, and G. Kalna for assistance with statistical methods. Cancer Research UK supported this work (grant C596/A17196).

Received: July 22, 2013
Revised: November 1, 2013
Accepted: January 28, 2014
Published: February 27, 2014

REFERENCES

Akira, S. (2003). Mammalian Toll-like receptors. Curr. Opin. Immunol. *15*, 5–11.

Balkwill, F. (2009). Tumour necrosis factor and cancer. Nat. Rev. Cancer *9*, 361–371.

Balkwill, F., and Mantovani, A. (2001). Inflammation and cancer: back to Virchow? Lancet *357*, 539–545.

Beutler, B., Hoebe, K., Du, X., and Ulevitch, R.J. (2003). How we detect microbes and respond to them: the Toll-like receptors and their transducers. J. Leukoc. Biol. *74*, 479–485.

Bilder, D. (2004). Epithelial polarity and proliferation control: links from the Drosophila neoplastic tumor suppressors. Genes Dev. *18*, 1909–1925.

Bilder, D., and Perrimon, N. (2000). Localization of apical epithelial determinants by the basolateral PDZ protein Scribble. Nature *403*, 676–680.

Bilder, D., Li, M., and Perrimon, N. (2000). Cooperative regulation of cell polarity and growth by Drosophila tumor suppressors. Science *289*, 113–116.

Brumby, A.M., and Richardson, H.E. (2003). scribble mutants cooperate with oncogenic Ras or Notch to cause neoplastic overgrowth in Drosophila. EMBO J. *22*, 5769–5779.

Colombani, J., Andersen, D.S., and Léopold, P. (2012). Secreted peptide Dilp8 coordinates Drosophila tissue growth with developmental timing. Science *336*, 582–585.

Cordero, J.B., Macagno, J.P., Stefanatos, R.K.A., Strathdee, K.E., Cagan, R.L., and Vidal, M. (2010). Oncogenic Ras diverts a host TNF tumor suppressor activity into tumor promoter. Dev. Cell *18*, 999–1011.

Doggett, K., Grusche, F.A., Richardson, H.E., and Brumby, A.M. (2011). Loss of the Drosophila cell polarity regulator Scribbled promotes epithelial tissue overgrowth and cooperation with oncogenic Ras-Raf through impaired Hippo pathway signaling. BMC Dev. Biol. *11*, 57.

Dow, L.E., Brumby, A.M., Muratore, R., Coombe, M.L., Sedelies, K.A., Trapani, J.A., Russell, S.M., Richardson, H.E., and Humbert, P.O. (2003). hScrib is a functional homologue of the Drosophila tumour suppressor Scribble. Oncogene *22*, 9225–9230.

Fernandez-Ayala, D.J.M., Sanz, A., Vartiainen, S., Kemppainen, K.K., Babusiak, M., Mustalahti, E., Costa, R., Tuomela, T., Zeviani, M., Chung, J., et al. (2009). Expression of the Ciona intestinalis alternative oxidase (AOX) in Drosophila complements defects in mitochondrial oxidative phosphorylation. Cell Metab. *9*, 449–460.

Ferrandon, D., Jung, A.C., Criqui, M., Lemaitre, B., Uttenweiler-Joseph, S., Michaut, L., Reichhart, J., and Hoffmann, J.A. (1998). A drosomycin-GFP reporter transgene reveals a local immune response in Drosophila that is not dependent on the Toll pathway. EMBO J. *17*, 1217–1227.

Froldi, F., Ziosi, M., Tomba, G., Parisi, F., Garoia, F., Pession, A., and Grifoni, D. (2008). Drosophila lethal giant larvae neoplastic mutant as a genetic tool for cancer modeling. Curr. Genomics *9*, 147–154.

Garelli, A., Gontijo, A.M., Miguela, V., Caparros, E., and Dominguez, M. (2012). Imaginal discs secrete insulin-like peptide 8 to mediate plasticity of growth and maturation. Science *336*, 579–582.

Goto, A., Kumagai, T., Kumagai, C., Hirose, J., Narita, H., Mori, H., Kadowaki, T., Beck, K., and Kitagawa, Y. (2001). A Drosophila haemocyte-specific protein, hemolectin, similar to human von Willebrand factor. Biochem. J. *359*, 99–108.

Hanahan, D., and Weinberg, R.A. (2011). Hallmarks of cancer: the next generation. Cell *144*, 646–674.

Hirabayashi, S., Baranski, T.J., and Cagan, R.L. (2013). Transformed Drosophila cells evade diet-mediated insulin resistance through wingless signaling. Cell *154*, 664–675.

Hoffmann, J.A. (1995). Innate immunity of insects. Curr. Opin. Immunol. *7*, 4–10.

Humbert, P.O., Grzeschik, N.A., Brumby, A.M., Galea, R., Elsum, I., and Richardson, H.E. (2008). Control of tumourigenesis by the Scribble/Dlg/Lgl polarity module. Oncogene *27*, 6888–6907.

Igaki, T., Pastor-Pareja, J.C., Aonuma, H., Miura, M., and Xu, T. (2009). Intrinsic tumor suppression and epithelial maintenance by endocytic activation of Eiger/TNF signaling in Drosophila. Dev. Cell *16*, 458–465.

Karin, M., and Greten, F.R. (2005). NF-kappaB: linking inflammation and immunity to cancer development and progression. Nat. Rev. Immunol. *5*, 749–759.

Kim, S., and Karin, M. (2011). Role of TLR2-dependent inflammation in metastatic progression. Ann. N Y Acad. Sci. *1217*, 191–206.

Lemaitre, B. (2004). The road to Toll. Nat. Rev. Immunol. *4*, 521–527.

Lemaitre, B., and Hoffmann, J. (2007). The host defense of Drosophila melanogaster. Annu. Rev. Immunol. *25*, 697–743.

Maruyama, K., Selmani, Z., Ishii, H., and Yamaguchi, K. (2011). Innate immunity and cancer therapy. Int. Immunopharmacol. *11*, 350–357.

Munier, A.I., Doucet, D., Perrodou, E., Zachary, D., Meister, M., Hoffmann, J.A., Janeway, C.A., Jr., and Lagueux, M. (2002). PVF2, a PDGF/VEGF-like

growth factor, induces hemocyte proliferation in Drosophila larvae. EMBO Rep. *3*, 1195–1200.

Pagliarini, R.A., and Xu, T. (2003). A genetic screen in Drosophila for metastatic behavior. Science *302*, 1227–1231.

Parisi, F., and Vidal, M. (2011). Epithelial delamination and migration: lessons from Drosophila. Cell Adhes. Migr. *5*, 366–372.

Pastor-Pareja, J.C., Wu, M., and Xu, T. (2008). An innate immune response of blood cells to tumors and tissue damage in Drosophila. Dis. Model. Mech. *1*, 144–154, discussion 153.

Ridley, E.V., Wong, A.C.N., and Douglas, A.E. (2013). Microbe-dependent and nonspecific effects of procedures to eliminate the resident microbiota from Drosophila melanogaster. Appl. Environ. Microbiol. *79*, 3209–3214.

Shia, A.K., Glittenberg, M., Thompson, G., Weber, A.N., Reichhart, J.-M., and Ligoxygakis, P. (2009). Toll-dependent antimicrobial responses in Drosophila larval fat body require Spätzle secreted by haemocytes. J. Cell Sci. *122*, 4505–4515.

Stern, C., and Bridges, C.B. (1926). The mutants of the extreme left end of the second chromosome of Drosophila melanogaster. Genetics *11*, 503–530.

Wood, W., Faria, C., and Jacinto, A. (2006). Distinct mechanisms regulate hemocyte chemotaxis during development and wound healing in Drosophila melanogaster. J. Cell Biol. *173*, 405–416.

Wu, M., Pastor-Pareja, J.C., and Xu, T. (2010). Interaction between Ras(V12) and scribbled clones induces tumour growth and invasion. Nature *463*, 545–548.

Zinke, I., Kirchner, C., Chao, L.C., Tetzlaff, M.T., and Pankratz, M.J. (1999). Suppression of food intake and growth by amino acids in Drosophila: the role of pumpless, a fat body expressed gene with homology to vertebrate glycine cleavage system. Development *126*, 5275–5284.